

Numerical Heat Transfer, Part A: Applications

An International Journal of Computation and Methodology

ISSN: (Print) (Online) Journal homepage: www.tandfonline.com/journals/unht20

Exploring novel heat transfer correlations: Machine learning insights for molten salt heat exchangers

Seyed Hamed Godasiaei & Ali J. Chamkha

To cite this article: Seyed Hamed Godasiaei & Ali J. Chamkha (27 Feb 2024): Exploring novel heat transfer correlations: Machine learning insights for molten salt heat exchangers, Numerical Heat Transfer, Part A: Applications, DOI: [10.1080/10407782.2024.2321524](https://doi.org/10.1080/10407782.2024.2321524)

To link to this article: <https://doi.org/10.1080/10407782.2024.2321524>



Published online: 27 Feb 2024.



Submit your article to this journal [↗](#)



View related articles [↗](#)



View Crossmark data [↗](#)



Exploring novel heat transfer correlations: Machine learning insights for molten salt heat exchangers

Seyed Hamed Godasiaei^a  and Ali J. Chamkha^b 

^aSchool of Chemical Engineering and Technology, Xi'an Jiaotong University, P.R. China; ^bFaculty of Engineering, Kuwait College of Science and Technology, Doha, Kuwait

ABSTRACT

The utilization of molten salts in heat transfer applications, specifically within shell-and-tube heat exchangers, has garnered significant attention for its potential in sustainable energy solutions. This study employs advanced machine learning algorithms, including decision tree regressor, support vector regressor, extreme gradient boosting, and random forest, to not only predict the heat transfer behavior of molten salts but also unravel the complex mechanisms underlying this process. Achieving a remarkable accuracy score of 0.985, the Support Vector Regressor leads the predictive models, closely followed by random forest (0.982), Decision Tree Regressor (0.974), and Extreme Gradient Boosting (0.965). The incorporation of Shapley Additive exPlanations values accentuates the Reynolds number's pivotal role, elucidating a robust correlation with the Nusselt value. These insights transcend mere prediction, offering a profound understanding that can significantly impact the design and optimization of molten salt heat exchangers. The applications of molten salts extend across various sectors, including concentrated solar energy and thermal storage, solidifying their position as a versatile and effective solution in the pursuit of sustainable and efficient energy systems.

ARTICLE HISTORY

Received 8 January 2024
Revised 13 February 2024
Accepted 16 February 2024

KEYWORDS

Molten salt; decision tree regressor; random forest; extreme gradient boosting; support vector regressor

1. Introduction

In recent years, the convergence of thermal sciences and machine learning has emerged as a key focus of research, offering innovative solutions to longstanding challenges in predicting and optimizing heat transfer processes [1,2]. The past decade has witnessed significant advancements in the efficacy and efficiency of machine learning models, leading to their widespread integration across diverse industries [3]. This integration goes beyond traditional applications, finding resonance in complex thermal systems where conventional methodologies encounter limitations [4]. Researchers have increasingly turned to machine learning algorithms to address intricate problems in heat transfer, including the prediction of heat transfer coefficients, thermal conductivity capacities, specific heat, and other critical parameters [5]. The distinguishing capability of machine learning models to identify intricate correlations and nonlinear patterns has proven superior to traditional curve-fitting techniques, driving their adoption [6]. The potential for reducing computational time in solving complex Computational Fluid Dynamics problems has made machine learning an integral part of scientific research in heat transfer [7]. Numerous scientific studies have undertaken experiments and numerical calculations focused on the performance of advanced molten salt thermal technology in simple circular tubes, heat exchangers, and

Nomenclature

ρ	Density [kg.m ⁻³]	<i>RBF</i>	Radial Basis Function
d	Diameter[m]	<i>SVR</i>	Vector regression
Nu	Nusselt number	<i>ReLU</i>	The Rectified Linear Unit
Pr	Prandtl number	<i>CFD</i>	Computational Fluid Dynamics
p	Pressure [N/m ²]	<i>ANN</i>	Artificial Neural Networks
$\Omega(f_k)$	Regularization term for each tree in the ensemble	<i>RF</i>	Random Forests
Re	Reynolds number	<i>XGBoost</i>	Extreme Gradient Boosting
T	Temperature [K]	<i>ML</i>	Machine learning
x_i	The input for the i -th training example	<i>GEP</i>	Genetic programming
N	The number of the pairs of <i>CFD</i> calculated and predicted values	<i>SHAP</i>	SHapley Additive exPlanations
K	The number of trees in the ensemble.		
T	The number of trees in the forest		
\hat{y}_i	The predicted target value for the i -th training example.	Greek symbol	
$h_i(x)$	The prediction of the i -th tree	θ	Represents the model parameters
y_i	The true target value for the i -th training example	Subscript	
		<i>avg</i>	Average
		n	The number of training examples

annular channels [8,9]. Notable findings include deviations in the Nusselt number in laminar and turbulent flow in horizontal tubes or heat exchangers under uniform heat flux conditions, indicating disparities from values calculated by classical heat transfer formulas [10–12]. Comparisons of the Nusselt number for molten salts, such as LiNO₃, FLiNaK, and HITEC, in transitional and turbulent flow with classical forced convection heat transfer correlations have demonstrated commendable agreement, with a maximum error of 20%. The viscosity of molten salt, particularly in laminar flow, has been identified as a factor influencing heat transfer [10, 13]. The use of machine learning has proven to be an effective method for reducing maximum errors in results obtained from traditional approaches. A pioneering study by Abbasi *et al.* [14] delves into the design of shell-and-tube heat exchangers incorporating segmental porous baffles. Employing computational fluid dynamics and machine learning, the research explores the thermo-hydraulic effects of these baffles on shell-side flow in an STHX. An artificial neural network is trained to predict the system's performance. This innovative STHX design holds the promise of simultaneous improvements in pressure drop rate and heat transfer, marking a significant enhancement in overall efficiency. Various machine learning models have been employed to predict specific thermal properties, yielding significant outcomes that have spurred further research. Wu *et al.* [15] predicted contact heat transfer between two solids using machine learning models, with LR and GBM models outperforming other algorithms. Jamei *et al.* [16] used machine learning to predict the specific heat capacity of molten salt, with the ETR model demonstrating superior results. Fan *et al.* [17] utilized SVM and XGBoost algorithms to predict solar radiation, with SVM showing slightly better results than the XGBoost model. Karimipour *et al.* [18] compared machine learning models for predicting the thermal conductivity of MWCNT-CuO/water hybrid nanofluid, revealing that the SVR model exhibited superior performance. Bang *et al.* [19] predicted the thermal conductivity of bentonite using different machine-learning models, emphasizing the superior performance of the GPR model. Marani and Nehdi [20] employed RF, DTR, and XGBoost models to predict the compressive strength of PCM-enhanced cement composites, with the gradient-boosting machine learning model demonstrating the highest accuracy. Zhu *et al.* [21] used XGBoost, RF, and ANN models to predict heat transfer coefficients, with ANN and XGBoost outperforming the RF model. Acikgoz *et al.* [22] utilized machine learning models to predict heat transfer coefficients for mixed and forced convection, finding that the ANN model showed

superior performance. Kwon *et al.* [23] used the RF model to predict the heat transfer coefficient of microchannels with surface roughness, achieving a high R_2 value of 0.966. Shahsavari *et al.* [24] employed the XGBoost algorithm to predict entropy production and liquid fraction for a heat sink, obtaining acceptable results with an R_2 value of 0.991 for the parameters. Alizadeh *et al.* [25] used SVR and ANN models to predict heat transfer in a hybrid nanofluid flow, achieving a substantial computational time savings of 90%.

This study presents a systematic inquiry into the potential utility of machine learning models as surrogates for computational fluid dynamics within the domain of heat transfer modeling, with a specific focus on molten salt shells and tube heat exchangers. Its principal objective is to assess the effectiveness of various machine learning methodologies in forecasting heat transfer outcomes, leveraging empirical data derived from experimental investigations. The deliberate selection of four prominent machine learning algorithms (Random Forest, Support Vector Regression, Decision Tree Regression, and XGBoost) underlines their relevance and efficacy in analogous domains. Through a meticulous application of these algorithms, the study elucidates their capability to accurately forecast heat transfer performance, thereby showcasing the extensive predictive capacities inherent in machine learning. The emphasis is placed on the inherent advantages of machine learning techniques, particularly their capacity to deliver precise predictions without entailing the computational complexities commonly associated with conventional numerical methodologies, such as solving partial differential equations. By demonstrating machine learning's adeptness in modeling intricate physical phenomena, the research advocates for a more streamlined and efficient approach to comprehending, predicting, and applying heat transfer principles in practical engineering contexts.

2. Machine learning modeling

2.1. A comprehensive exploration of the random forest algorithm

In the ever-evolving landscape of machine learning, the random forest algorithm stands out as a stalwart, acclaimed for its versatility and prowess in tackling both classification and regression challenges [26]. Rooted in the concept of ensemble learning, Random Forest leverages the collective wisdom of multiple decision trees to provide robust solutions to complex problems. At its core, Random Forest is a supervised learning algorithm, meaning it requires labeled training data to make informed predictions. It has become a cornerstone in machine learning applications, particularly for tasks where accuracy and problem-solving acumen are paramount. The metaphorical “forest” in Random Forest is not just a whimsical term; it encapsulates the essence of the algorithm's strength. Like a vibrant ecosystem thriving with diverse flora, a random forest comprises numerous decision trees [27]. The power of this algorithm lies in the sheer number of trees it assembles. As the forest grows, so does its robustness; an increasing number of trees enhances its accuracy and problem-solving capabilities. Each decision tree within the Random Forest is a classifier in its own right, trained on a distinct subset of the dataset. This diversity is intentional, introducing variability into the learning process [28]. The algorithm does not rely on the wisdom of a single tree but harnesses the collective insights of many. To arrive at a prediction, the Random Forest takes the average (for regression problems) or the majority vote (for classification tasks) of the predictions from individual decision trees [29]. This ensemble approach significantly contributes to improved predictive accuracy. Central to the Random Forest's success is the concept of ensemble learning. Ensemble learning is a strategic amalgamation of multiple classifiers to address intricate problems and elevate the overall performance of the model. Random Forest epitomizes this concept, orchestrating a harmonious collaboration of decision trees to navigate the complexities inherent in diverse datasets (As illustrated in Figure 1). In this algorithmic symphony, the strength lies not only in the individual trees but in their collective wisdom. The more

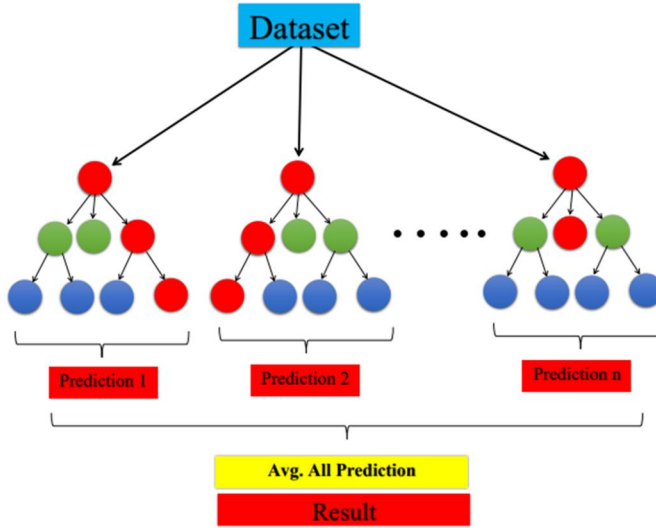


Figure 1. Schematic diagram of the random forest regression tree model.

trees in the Random Forest, the richer and more robust its predictive capabilities become. As we delve deeper into the intricacies of Random Forest, we unveil a sophisticated tool in the machine learning arsenal, ready to decipher patterns, solve challenges, and propel us into a realm of enhanced predictive modeling.

2.2. A comprehensive exploration of the extreme gradient boosting algorithm

In the dynamic landscape of machine learning, XGBoost stands out as a pivotal force; a meticulously designed, highly optimized distributed gradient boosting library meticulously crafted for the efficient and scalable training of ML models. Positioned as a frontrunner in ensemble learning, XGBoost adeptly consolidates predictions from multiple weak models, delivering outcomes of heightened robustness and precision [30]. The nomenclature, “Extreme Gradient Boosting” (XGBoost), underscores its commitment to advancing the forefront of gradient boosting techniques. Renowned for unparalleled versatility, XGBoost has solidified its status as one of the most esteemed and extensively utilized machine learning algorithms. Its widespread adoption is fueled by exceptional proficiency in navigating vast datasets with finesse, excelling across a spectrum of machine learning tasks from classification to regression [31]. A distinctive feature setting XGBoost apart is its adept handling of missing values, endowing it with the capability to seamlessly traverse real-world datasets fraught with missing values. This proficiency obviates the need for arduous and extensive pre-processing, streamlining the modeling pipeline. Additionally, XGBoost boasts built-in support for parallel processing; a pivotal feature expediting model training on substantial datasets within reasonable timeframes [32]. This amalgamation of features positions XGBoost as an indispensable instrument for practitioners seeking high-performance machine-learning solutions. Its prowess becomes particularly evident in scenarios entailing extensive and intricate datasets, where XGBoost stands as a beacon of efficiency and reliability, setting a new standard in sophisticated machine-learning applications. Zooming into XGBoost Regression, it emerges as a notable ensemble algorithm, following the boosting process. Setting itself apart, XGBR represents an optimized Gradient Boosting algorithm where the loss function is normalized, strategically mitigating model variances and curtailing the risk of overfitting [33,34]. A noteworthy departure from traditional Gradient Boosting lies in XGB’s utilization of the Taylor expansion to augment the loss function, in contrast to Gradient Boosting, which solely

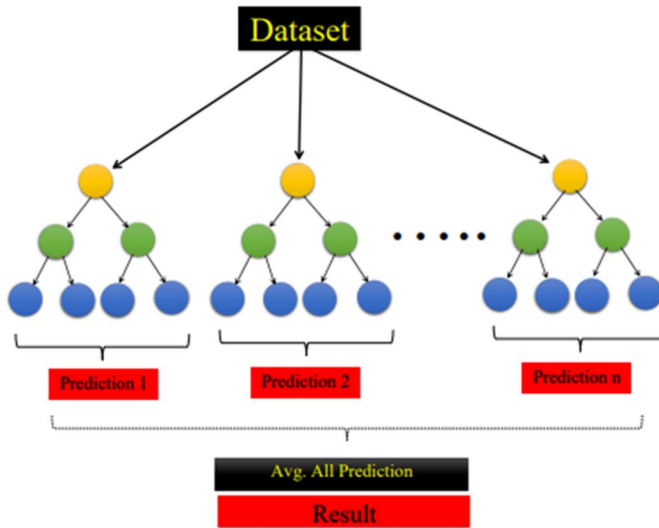


Figure 2. Schematic diagram of the XGBoost regression tree model.

considers the first derivative. The introduction of the Taylor expansion enhances the precision of the model, contributing to a more refined and accurate learning process. In the XGBR model, the ultimate prediction at each step (t) is derived from the sum of predictions made by each estimator (As illustrated in Figure 2). This summation, expressed by a specific equation, encapsulates the collective insight of individual estimators, culminating in the model's final prediction. This nuanced approach not only underscores the intricacies of the XGBR algorithm but also highlights its effectiveness in leveraging ensemble learning to achieve precise and robust predictions.

2.3. A Comprehensive Exploration of the decision tree regression algorithm

In the expansive domain of machine learning, decision tree regression stands as a potent algorithm meticulously crafted to unravel the intricacies of predicting continuous numerical values. Distinct from its classification counterpart, Decision Tree Regression immerses itself in the domain of regression tasks, where the objective transcends assigning categorical labels to forecast outcomes along a continuous scale [35]. This algorithm occupies a central role in the ensemble of tools harnessed for predictive modeling, presenting a distinctive fusion of interpretability and versatility. At its fundamental core, decision tree regression artfully constructs a tree-like structure where each branch and leaf encapsulates pivotal decision points and corresponding predicted values (As illustrated in Figure 3). The process of building this tree involves astutely selecting features and split points to strategically minimize variance within the resulting subsets [36]. The allure of this algorithm is underscored by its innate interpretability; the resulting tree serves as a visual narrative, unfolding the conditions leading to precise predictions. A salient characteristic of decision tree regression is its remarkable adaptability, proficiently handling both categorical and numerical data [37]. This versatility positions it as a stalwart across a spectrum of applications, finding utility in scenarios ranging from predicting housing prices and stock values to estimating any continuous numerical outcome. However, like any robust tool, decision tree regression encounters challenges, with overfitting being a prominent concern. Mitigation strategies such as pruning and the strategic imposition of constraints during the tree-building process act as vigilant guardians, preventing the emergence of an overly intricate structure that might excessively align with the intricacies of the training data. Embarking on an exploration of decision tree regression reveals a realm where interpretability converges with predictive precision. The branching

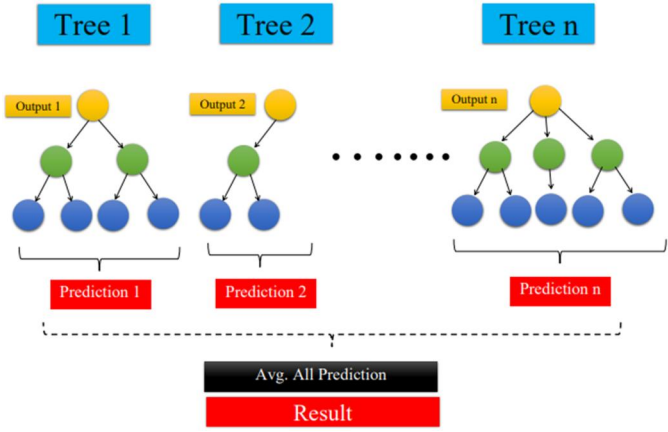


Figure 3. Schematic diagram of the DTR regression tree model.

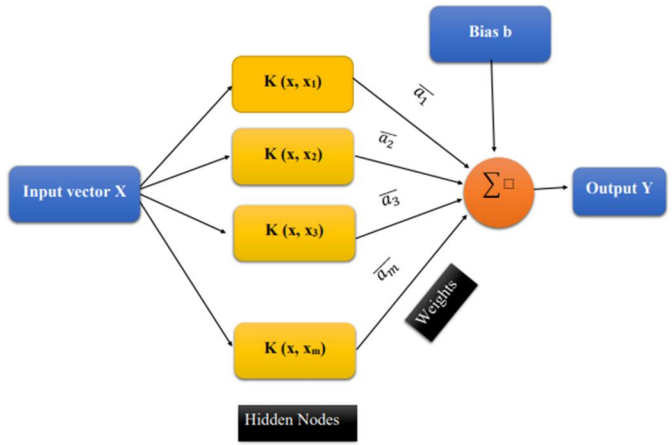


Figure 4. Schematic diagram of the SVM regression tree model.

decisions of the algorithm pave the way for insightful forecasting, navigating the continuum of numerical outcomes with finesse. In essence, decision tree regression emerges not just as an algorithm but as a guiding beacon in the pursuit of understanding and predicting continuous numerical values.

2.4. A comprehensive exploration of the support vector regression algorithm

Support vector regression stands as a sophisticated and robust machine learning algorithm specifically designed to address regression tasks with a focus on predicting continuous output values. Diverging from its classification counterpart, SVR assumes a pivotal role in scenarios where the target variable exists on a continuous scale, making it an invaluable tool for precise and nuanced predictions [36]. At its core, SVR leverages the foundational principles of support vector machines, strategically seeking an optimal hyperplane within a high-dimensional space. This hyperplane serves the crucial purpose of partitioning data into distinct classes (as illustrated in Figure 4). However, SVR distinguishes itself by shifting the emphasis from classification to regression. Its primary objective is to maximize the margin between the identified hyperplane and the nearest data points of each class while simultaneously minimizing errors associated with

predicting continuous values. One of the distinctive strengths of SVR lies in its adaptive nature, allowing it to proficiently handle both linear and non-linear regression challenges [38]. This adaptability is achieved through the incorporation of diverse kernel functions. The linear kernel, characterized by a simple dot product, excels at capturing linear relationships within the data. In contrast, non-linear kernels, such as the Radial Basis Function kernel, come into play when dealing with intricate patterns present in complex datasets. The applications of SVR span a broad spectrum, encompassing domains such as time series forecasting, financial trend prediction, and biomedical research. Its utility becomes evident in scenarios where the precision of predictions for continuous values is paramount. This formal overview serves as a prelude to a comprehensive exploration of SVR, shedding light on its theoretical underpinnings, its adaptability through kernel selection, and its impactful applications across diverse real-world contexts.

3. A comprehensive exploration of machine learning methodology

3.1. Efficient methods for gathering data, extracting features, and preparing information for machine learning

In the realm of thermal sciences, investigating the convective heat transfer of molten salt within shell and tube heat exchangers holds significant practical implications. Employing a multidisciplinary approach, advanced machine learning techniques; specifically, XGBoost, Random Forest, Decision Tree Regression, and Support Vector Regression; take center stage as instrumental tools for unraveling and predicting the intricate dynamics of heat transfer. At the core of this research lies a meticulously curated dataset, comprising 170 data samples meticulously extracted from empirical articles [39–42]. This dataset encompasses ten crucial features, with nine serving as input variables and the tenth representing the output variable. The intricacies of these features, their interdependencies, and their collective impact on the overarching heat transfer process are comprehensively elucidated in Table 1. To construct robust and predictive models, the dataset undergoes strategic partitioning into "training" and "testing" subsets. Approximately 85% of the data is dedicated to the training set, leaving the remaining 15% for meticulous testing (As illustrated in Figure 5). Rigorous measures are implemented to ensure consistency in training and testing examples across all developed machine-learning models. This consistency is achieved through the application of a unique "random mode," facilitated by the scikit-learn package in Python. This approach ensures that each model encounters a comparable set of training and testing instances, fostering fair and rigorous evaluations. The utilization of machine learning methodologies, coupled with a well-structured dataset, positions this research at the forefront of unraveling the complexities inherent in molten salt convective heat transfer within shell and tube heat exchangers.

3.2. Advancements in machine learning: model development, hyperparameter tuning, and cross-validation strategies

In the endeavor to optimize the performance of the algorithms utilized in this study, a systematic methodology was embraced. This involved the integration of a dual-pronged approach

Table 1. Input and output features of the dataset prepared for this study.

No.	Characteristic	Unite	Subscript	No.	Characteristic	Unite	Subscript
1	Length of tube	m	L	6	Type of Baffle	-	<i>Baffle</i>
2	Number of tube	-	n_t	7	Number of Baffles	-	n_b
3	Outer diameter of tube	m	d_t	8	Minimum temperature	$^{\circ}\text{C}$	T_{min}
4	Outer diameter of shell	m	d_s	9	Maximum temperature	$^{\circ}\text{C}$	T_{max}
5	Reynolds	-	Re	10	Nusselt	-	Nu

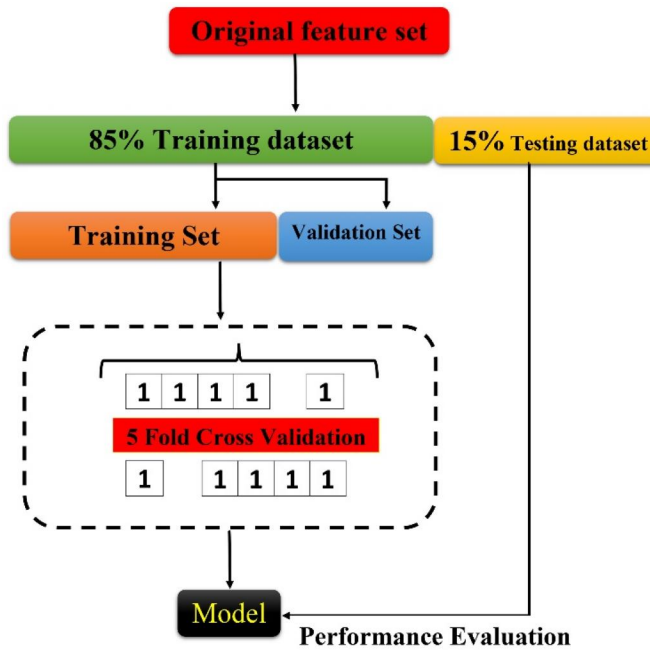


Figure 5. The schematic diagram of the fivefold cross-validation.

comprising fivefold cross-validation and a stepwise-randomized searching algorithm to fine-tune the hyperparameters of each Algorithm [43]. The orchestration of this optimization process was achieved through the utilization of the “RandomizedSearchCV” class embedded within the scikit-learn library. The “RandomizedSearchCV” class offers both “fit” and “score” methods, with additional support for “score_samples,” “predict,” “predict_proba,” “decision_function,” “transform,” and “inverse_transform” if implemented in the estimator used. This class facilitates the optimization of the parameters of the estimator through a cross-validated search over specified parameter settings [44]. Notably, unlike GridSearchCV, RandomizedSearchCV does not attempt all possible parameter values. Instead, it samples a fixed number of parameter settings from specified distributions, with the number of settings determined by the parameter “n_iter.” Within the framework of k-fold cross-validation, the dataset is methodically divided into k subsets or folds. The model is then iteratively fitted to the data k times, with k-1 folds employed for training in each iteration, and the kth fold serving as the test data. This iterative process ensures a comprehensive evaluation of the model’s performance across diverse subsets of the dataset, enhancing the robustness of the model [45]. Figure 5 provides a visual depiction of the schematic structure of a fivefold cross-validation, illustrating the sequential training and testing phases. It is pertinent to acknowledge that each machine-learning algorithm features unique parameters. To augment the accuracy of predicted outputs, the study meticulously fine-tuned these parameters, tailoring them to the specific characteristics of each machine-learning algorithm. This thorough tuning process was designed to extract optimal configurations for the models, ultimately contributing to more precise and reliable predictions.

3.3. Evaluating model performance: metrics and strategies in machine learning

In the rigorous evaluation of the precision of the employed machine learning methodologies, a comprehensive suite of fundamental statistical metrics is strategically employed. Consistent with

established norms in the scholarly literature, these metrics serve as a uniform and standardized apparatus for discerning the efficacy of the models across diverse dimensions [46–49]. The ensuing elucidation provides a detailed account of each evaluative criterion.

$$R^2 = 1 - \frac{\sum_{i=1}^n (y_i - \hat{y}_i)^2}{\sum_{i=1}^n (y_i - \bar{y})^2} \quad (1)$$

The R^2 -value emerges as a pivotal metric, offering profound insights into the degree to which the model expounds the variability within the observed data. Spanning a range from 0 to 1, a heightened R^2 -value signifies an augmented capacity for explanatory power, underscoring the model's adeptness in capturing and revealing latent patterns within the data.

$$MSE = \frac{1}{n} \sum_{i=1}^n (\hat{y}_i - y_i)^2 \quad (2)$$

$$RMSE = \sqrt{\frac{1}{n} \sum_{i=1}^n (\hat{y}_i - y_i)^2} \quad (3)$$

Serving as a complement to MSE, RMSE denotes the square root of the mean squared error. This measure provides an assessment of the average magnitude of errors, imparting an understanding of the typical size of prediction errors. Lower RMSE values are emblematic of elevated model accuracy and precision.

$$MAE = \frac{1}{n} \sum_{i=1}^n |\hat{y}_i - y_i| \quad (4)$$

MAE, through its calculation of the mean absolute difference between predicted and observed values, furnishes a direct appraisal of the model's overall precision. Diminished MAE values signal superior performance, particularly in terms of minimizing absolute prediction errors.

Collectively, these metrics furnish a standardized and quantitative framework meticulously tailored for the evaluation of the predictive capabilities inherent in machine learning models. The comprehensive consideration of multiple facets of predictive accuracy, spanning explanatory power, precision, and error magnitudes, imbues these assessments with the nuance required for a discerning comprehension of the reliability and efficacy of the applied machine learning techniques. The strategic amalgamation of these metrics ensures a thorough and holistic evaluation, transcending singular measures and providing a well-rounded perspective on the models' performance.

4. Results and discussions

4.1. Optimizing model performance: a comprehensive guide to Hyperparameter tuning in machine learning

In the field of machine learning, hyperparameters serve as predefined settings that exert control over a model's training process and behavior. Distinct from parameters learned from training data, the intelligent selection of hyperparameters is paramount, directly influencing model performance, its ability to generalize to new data, and its susceptibility to overfitting. When considering specific machine learning algorithms, such as Random Forest, pivotal meta-parameters like the number of trees (`n_estimators`), minimum samples required for node splitting (`min_samples_split`), and maximum tree depth (`max_depth`) play a central role in shaping model complexity and diversification. Strategically tuning these meta-parameters proves instrumental in preventing overfitting and enhancing generalization. Similarly, for the XGBoost algorithm, meticulous fine-tuning of meta-parameters, including learning rate, boosting rounds (`n_estimators`), and individual tree depth (`max_depth`), is imperative to strike a balance between model accuracy and

Table 2. Hyperparameters for the employed machine learning algorithms in this study.

No	Algorithms	Hyperparameters
1	<i>RF</i>	"n_estimators" = 100; "min_samples_split" = 5; "min_samples_leaf" = 2; "max_depth" = 10; "max_features" = log2.
2	<i>XGBoost</i>	"n_estimators" = 100; "min_child_weight" = 3; "learning_rate" = 0.1; "colsample_bytree" = 0.8; "colsample_bylevel" = 0.8; "max_depth" = 10.
3	<i>DTR</i>	"max_depth"=None; "min_samples_split"=2; "min_samples_leaf"=1.
4	<i>SVR</i>	"Kernel"=linear ; "gamma"=auto; "epsilon"=0.1.

computational efficiency. In the realm of Decision Tree Regression, meta-parameters such as maximum tree depth (`max_depth`), minimum samples for node splitting (`min_samples_split`), and minimum samples in a leaf node (`min_samples_leaf`) directly influence structural complexity. Deliberate adjustments of these hyperparameters are essential for managing the delicate tradeoff between model complexity and overfitting. For Support Vector Regression, key meta-parameters include the tuning parameter, determining the balance between fitting training data and maintaining a smooth decision boundary. The choice of kernel type (`kernel`) and kernel coefficient (`gamma`) further shapes model flexibility and complexity. Methodological fine-tuning of these meta-parameters is requisite for achieving optimal regression performance. Acting as modifiable elements, hyperparameters empower practitioners to tailor machine learning models to the unique characteristics of their datasets. The process of meta-parameter optimization involves systematic exploration to pinpoint the configuration that maximizes the model's performance on unseen data, ensuring its suitability and efficiency for the designated task. Table 2 displays the fine-tuned parameters for the four employed algorithms.

4.2. An in-depth exploration: unraveling the predictive performance of machine learning algorithms

Residuals within the framework of regression modeling delineate the disparity between observed values and the corresponding predictions generated by the model. A meticulous analysis of residuals yields valuable insights into the model's efficacy in capturing inherent patterns within the dataset. Illustratively, in the instance of a random forest model, residuals embody the distinction between actual target values and predictions crafted by amalgamating decision trees constituting the random forest. Given the amalgamation of multiple decision trees in Random Forest, residuals encapsulate the cumulative error of the entire ensemble, as depicted in Figure 6a. Similarly, in decision tree regression, residuals portray the variability between observed target values and predictions derived from an individual decision tree, functioning as an indicator of how adeptly the singular decision tree captures patterns in the data (As demonstrated in Figure 6b). Transitioning to SVR, this methodology seeks to ascertain a hyperplane that optimally fits the data while minimizing errors, as evident in Figure 6c. Residuals manifest in SVR as vertical deviations between observed values and the hyperplane. Scrutinizing SVR residuals facilitates an assessment of the hyperplane's fidelity in representing underlying relationships in the dataset. In the same vein, within the domain of XGBoost, mirroring random forest as an ensemble learning approach, XGBoost residuals differentiate actual target values from predictions amalgamated by the boosted ensemble of weak learners, typically trees (as anticipated in Figure 6d. XGBoost operates iteratively to rectify errors introduced by preceding weak learners in each iteration, thereby enhancing its predictive accuracy.

The investigation into convective heat transfer involving triple nitrate salt in diverse shell and tube heat exchangers is a comprehensive exploration of the thermal dynamics and efficiency of these systems. It delves into the intricate process of heat exchange between triple nitrate salt and the surrounding environment within various heat exchanger configurations, examining key

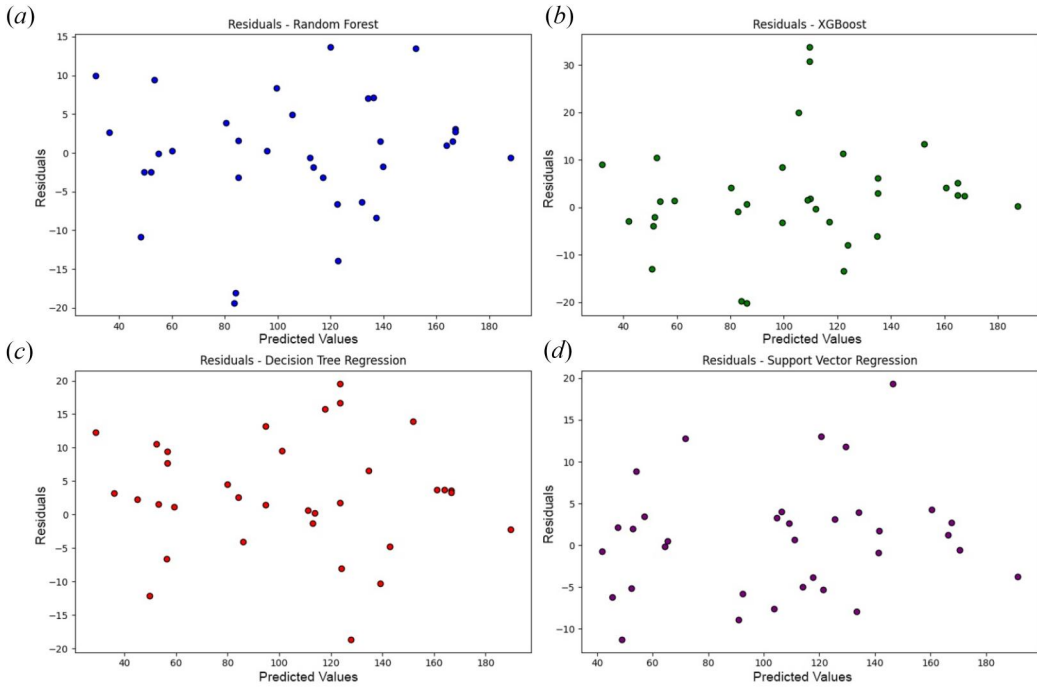


Figure 6. Analyzing model residuals: a comparative study across random forest, decision tree regression, SVR, and XGBoost.

Table 3. Statistical error metrics across machine learning algorithms.

No.	Algorithms	MAE (MPa)	RMSE (MPa)	MSE (MPa)	R^2 -values
1	RF	2.15	2.62	6.91	0.982
2	XGBoost	2.63	3.64	13.25	0.965
3	DTR	2.49	3.19	10.17	0.974
4	SVR	2.11	2.39	5.72	0.985

parameters such as Reynolds and Nusselt numbers, tube length, number of tube, tube diameter, shell diameter, number of baffles, temperature range, and the type of baffle. The research includes a thorough analysis of the Reynolds number across a range from 500 to 20000. Employing machine learning techniques to process experimental data and predict Nusselt numbers yielded results closely aligned with those from experimental articles, highlighting a remarkable consistency between the two approaches. The statistical evaluation of machine learning models, including RF, DTR, SVR, and XGBoost, is presented in Table 3, encompassing metrics such as MSE, RMSE, MAE, and accuracy. The reported high accuracy of these models underscores the effectiveness of the modeling approach in capturing the complexities of convective heat transfer involving triple nitrate salt.

In the realm of modeling and statistical analysis, the role of residuals is crucial, representing the differences between observed and predicted values. This disparity is systematically depicted against predicted values or relevant variables to gauge the efficacy of the models. Figure 7a visually presents the mean residual plot for the RF, DTR, SVR, and XGBoost algorithms. Conversely, Figure 7b elucidates the mean residual plot, offering insight into the average values of residuals across various levels of predicted values. This graphical representation aids in discerning potential systematic biases within the models, indicating whether the residuals consistently overestimate or underestimate the true values. In an ideal residual plot, differences between observed and predicted values ideally manifest as a random pattern without any recognizable trend. This ideal scenario signifies that the models adeptly capture the underlying patterns in the data, with

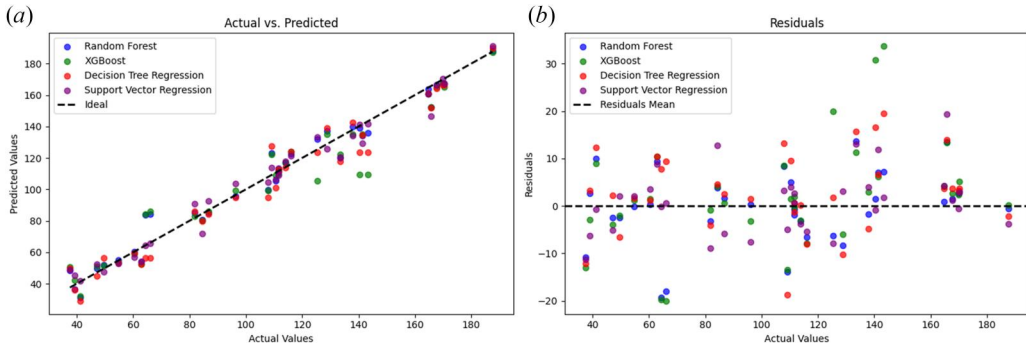


Figure 7. Diagnostic plots: assessing model performance through mean and ideal residuals.

residuals uniformly distributed around zero. The absence of a discernible trend implies that the models perform optimally in representing the intricacies inherent in the dataset.

The in-depth analysis of four prominent machine learning models, namely DTR, SVR, XGBoost, and RF, reveals subtle differences in their predictive accuracies, shedding light on their respective strengths. The SVR model takes the lead by exhibiting the highest accuracy score of 0.985, signifying its exceptional ability to make precise predictions. Close on its heels, the RF model performs commendably with an accuracy of approximately 0.982, positioning itself as a robust contender closely aligned with the high-performing SVR model. The DTR algorithm also proves its mettle with a noteworthy accuracy of 0.974, while the XGBoost algorithm demonstrates solid performance with an accuracy of 0.965. Digging deeper into the Mean Absolute Error analysis, the SVR model distinguishes itself by yielding the lowest value of 2.11. This signifies that, on average, the SVR model's predictions deviate minimally from the actual values, showcasing a high degree of accuracy and resilience to outliers. This observation is further reinforced in the Root Mean Squared Error analysis, where the SVR model excels in minimizing errors, especially larger ones, as evidenced by its lowest RMSE value of 2.39.

4.3. Understanding the dynamics of feature importance in machine learning using SHAP values

In the intricate realm of machine learning models, grasping the factors that wield substantial influence over predictions is vital for both model interpretability and decision-making. Feature importance analysis assumes a pivotal role in demystifying the complexity inherent in these models, casting light on the specific contributions of each input variable to the ultimate outcomes. Amidst the array of methodologies designed for assessing feature importance, SHAP values have emerged as a potent and widely embraced approach. As machine learning models evolve in sophistication, their internal mechanisms often veer toward opacity, presenting a challenge in terms of interpretation. SHAP values confront this challenge head-on by providing a unified framework to quantify the impact of each feature on model predictions. Grounded in cooperative game theory, SHAP values equitably distribute the contribution of each feature across all possible combinations, yielding a more nuanced and comprehensive comprehension of how individual features exert their influence on predictions. At the core of SHAP values lies the concept of Shapley values, drawn from cooperative game theory. Shapley values allocate a just share of a coalition's overall contribution to each participant, ensuring that each contributor receives appropriate recognition for their unique input. In the context of machine learning, SHAP values adapt this concept to attribute the disparity between a model's output for a specific instance and the average prediction across all instances to each feature. This methodology provides a transparent and

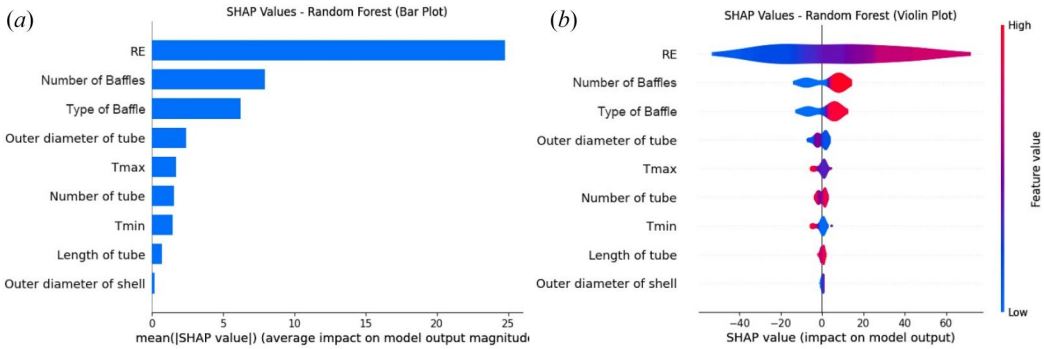


Figure 8. Machine learning insights on heat transfer of molten salt in heat exchangers: Exploring Reynolds number, number of Baffle, type of Baffle, tube diameter, maximum Temperature, number of tubes, minimum Temperature, tube length, and shell diameter.

equitable means to dissect the contribution of each feature to the overall predictive power of the model.

Figure 8 presents a comprehensive exploration of diverse parameters' impact on heat transfer and Nusselt number in molten salt shell and tube heat exchangers, leveraging machine learning perspectives. This analysis places a specific emphasis on the critical factors of Reynolds number, Number of Baffle, Type of Baffle, Diameter of tube, Temperature differentials, Number of tubes, Length of tube, and Diameter of shell. In Figure 8a, the preeminent influence is attributed to the Reynolds number, demonstrating a discernible correlation with the Nusselt value. As the Reynolds number escalates, a corresponding augmentation in the Nusselt number is observed. Following closely, the number of baffles and their geometric variations are acknowledged as influential factors, albeit with a less pronounced impact compared to the Reynolds number. The observed correlation between the Reynolds number, baffle characteristics, and their geometry suggests that the introduction of baffles plays a pivotal role in altering fluid flow patterns, inducing turbulence, enhancing mixing, and directing the flow. These modifications intricately impact both inertial and viscous forces, contributing collectively to the Reynolds number. The consequential increase in turbulence and fluid velocity yields higher inertial forces, thus elevating the Reynolds number. In strategic applications like heat exchangers, where heightened Reynolds numbers are indicative of enhanced heat transfer efficiency, the deliberate manipulation of baffles emerges as a key design choice. Turning attention to tube diameter within the shell and tube heat exchanger, its influence on heat transfer and the Nusselt number is salient, albeit relative to the configuration and number of baffles. Larger tube diameters afford increased surface area for heat transfer, facilitating efficient thermal exchange between fluids within the tube and the shell. Moreover, a larger diameter extends the contact time between fluids, augmenting heat energy transfer. The number of heat exchanger tubes becomes a pivotal parameter, as the dimensionless Nusselt number governs convective heat transfer. Alterations in tube diameter manifest in varied flow patterns, impacting velocity distribution and, consequently, the Nusselt number. Consideration of the fluid's minimum and maximum temperatures becomes imperative, influencing the Nusselt number with correlations to different heat transfer regimes. The Nusselt number's expression in terms of experimental correlations is sensitive to temperature profiles and differences, thereby affecting the flow regime. Increasing the diameter of the shell within the heat exchanger emerges as a key factor in amplifying the Nusselt number. This augmentation results in a larger surface area, thereby enhancing heat transfer efficiency and fostering more substantial thermal energy exchange. However, the effect of shell diameter is acknowledged as relatively insignificant in comparison to other critical parameters and may be deemed negligible in specific cases when juxtaposed against more vital factors.

Figure 8 offers a nuanced and interconnected perspective on the intricate dynamics influencing heat transfer and the Nusselt number in molten salt shell and tube heat exchangers. This analysis underscores the importance of considering a multitude of factors for a holistic understanding and optimization of system performance.

4.4. Comparative analysis of Nu predictions: Machine learning approaches using SVR, DTR, RF, and XGBoost

The burgeoning interest in the utilization of molten salts for heat transfer applications, particularly within shell and tube heat exchangers, is grounded in their perceived potential to contribute significantly to sustainable energy solutions. This study embarks upon a comprehensive analysis, employing four distinct machine learning algorithms—Support Vector Regression, XGBoost, Random Forest, and Decision Tree Regression. A meticulous examination of parameters, meticulously detailed in Table 1, was conducted using these machine learning models. Figure 9 visually articulates a nuanced comparison between the outcomes derived from artificial neural network algorithms and experimental results for Nu. It is noteworthy that the results from all four

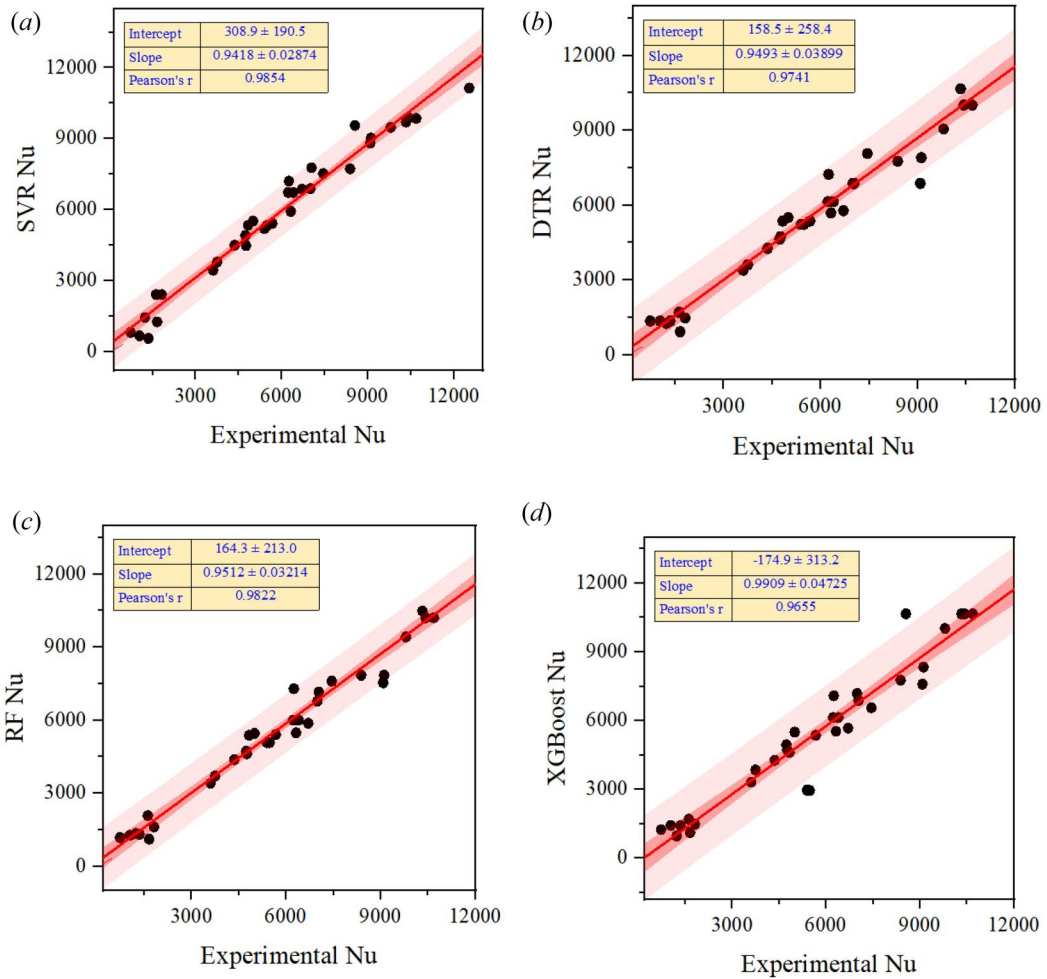


Figure 9. Illustrates the comparison between machine learning-predicted Nu and experimentally computed Nu using SVR, DTR, RF, and XGBoost.

algorithms exhibit a remarkable concordance with the experimental data, underscoring their capacity to faithfully model the considered heat transfer phenomena. Of particular significance is the outstanding performance of the SVR and RF models, evidenced by a significant coefficient of determination (R_2) of 0.98, as demonstrated in [Figures 9a and c](#). This underscores their commendable predictive prowess in evaluating relevant heat transfer phenomena. [Figures 9b and d](#) illustrate that DTR and XGBoost models display minimal deviations and closely align with experimental results. The mean absolute error is computed at 2.11 and 2.15 for SVR and RF models, respectively, serving as a metric providing insights into the overall accuracy of forecasts. Additionally, this study employs the root mean square error as a critical evaluation criterion for regression models, with SVR and RF models demonstrating an RMSE of 2.3 and 2.6, contributing to a deeper understanding of forecasting accuracy. The results, as depicted in [Figure 9](#), underscore the commendable accuracy and performance of SVR and RF models, suggesting their potential as a credible alternative to traditional computational fluid dynamics methods. This study positions these machine learning models as effective and precise tools for predicting experimental results in the field of heat transfer applications, offering a promising alternative to conventional methods and marking a significant advancement in this field.

5. Conclusions

In the pursuit of sustainable and efficient energy solutions, molten salts have emerged as a highly promising heat transfer fluid, finding versatile applications in concentrated solar energy and thermal energy storage. Understanding the intricacies of heat transfer characteristics in complex heat exchanger geometries is crucial for unleashing the full potential of molten salt. Among various configurations, shell and tube heat exchangers, renowned for their versatility, hold significance in this context. This article initiates a comprehensive review of molten salt heat transfers within the domain of shell and tube heat exchangers, aiming to explore the complexities of this dynamic heat exchange phenomenon. The study employs machine learning methodologies to conduct a broad exploration, scrutinizing various conditions and key parameters, such as Reynolds and Nusselt numbers, tube length, number of tubes, tube diameter, shell diameter, and the number of baffles. As molten salt technology progresses toward industrial implementation, the insights gleaned from this research are expected to significantly contribute to the design, optimization, and operational understanding of heat exchangers handling molten salt. This study uses four well-known machine learning algorithms for predictive modeling: DTR, SVR, XGBoost, and RF. It recognizes the promise of machine learning as an alternative to traditional methods. The integration of SHAP further enhances result interpretability, providing a detailed understanding of the complex interplay between variables. This study not only aims to predict heat transfer behavior but also seeks to elucidate the underlying mechanisms influencing molten salt heat transfer in shell and tube heat exchangers using advanced machine learning techniques. The outcomes derived from this research are outlined as follows:

- The comprehensive examination reveals the SVR model as the top performer, achieving the highest accuracy score of 0.985. This underscores its exceptional predictive precision, positioning it as the preferred choice among the array of machine learning models scrutinized. Additionally, the SVR model excels in Mean Absolute Error, yielding the lowest value of 2.11. This suggests minimal deviation on average between its predictions and actual values, emphasizing its accuracy and resilience to outliers.
- The Random Forest model exhibits commendable performance, with an accuracy close to 0.982. Its robustness positions it as a strong contender, matching the high-performance Support Vector Regression model and showcasing versatility.

- The Reynolds number emerges as the preeminent influencer, exhibiting a discernible correlation with the Nusselt value. As the Reynolds number increases, a corresponding augmentation in the Nusselt number is observed, signifying enhanced heat transfer efficiency.
- The number of baffles and their geometric variations are acknowledged as influential factors, albeit with a less pronounced impact compared to the Reynolds number. Baffles play a pivotal role in altering fluid flow patterns, inducing turbulence, and enhancing mixing, contributing collectively to the Reynolds number.
- Tube diameter within the shell and tube heat exchanger influences heat transfer and the Nusselt number, with larger diameters affording increased surface area for efficient thermal exchange. The number of heat exchanger tubes is pivotal, impacting flow patterns and the Nusselt number.
- Increasing the diameter of the shell within the heat exchanger amplifies the Nusselt number, enhancing heat transfer efficiency. However, the effect of shell diameter is relatively insignificant compared to other critical parameters and may be deemed negligible in specific cases.

Disclosure statement

No potential conflict of interest was reported by the authors.

ORCID

Seyed Hamed Godasiaei  <http://orcid.org/0000-0003-3575-8906>

Ali J. Chamkha  <http://orcid.org/0000-0002-8335-3121>

References

- [1] M. Zou, W. G. Jiang, Q. H. Qin, Y. C. Liu and M. L. Li, "Optimized XGBoost model with small dataset for predicting relative density of Ti-6Al-4V parts manufactured by selective laser melting," *Materials (Basel)*, vol. 15, no. 15, pp. 5298, 2022. DOI: [10.3390/ma15155298](https://doi.org/10.3390/ma15155298).
- [2] G. S. Sestito, R. Álvarez-Briceño, G. Ribatski, M. M. da Silva and L. P. R. de Oliveira, "Vibration-based multiphase-flow pattern classification via machine learning techniques," *Flow Meas. Instrum.*, vol. 89, pp. 102290, 2023. DOI: [10.1016/j.flowmeasinst.2022.102290](https://doi.org/10.1016/j.flowmeasinst.2022.102290).
- [3] W. Liu, Z. Chen and Y. Hu, "XGBoost algorithm-based prediction of safety assessment for pipelines," *Int. J. Press. Vessel. Pip.*, vol. 197, pp. 104655, 2022. DOI: [10.1016/j.ijpvp.2022.104655](https://doi.org/10.1016/j.ijpvp.2022.104655).
- [4] J. Mohammadpour, S. Husain, F. Salehi and A. Lee, "Machine learning regression-CFD models for the nanofluid heat transfer of a microchannel heat sink with double synthetic jets," *Int. Commun. Heat Mass Transf.*, vol. 130, pp. 105808, 2022. DOI: [10.1016/j.icheatmasstransfer.2021.105808](https://doi.org/10.1016/j.icheatmasstransfer.2021.105808).
- [5] Y. Kim and Y. Kim, "Explainable heat-related mortality with random forest and SHapley Additive exPlanations (SHAP) models," *Sustain. Cities Soc.*, vol. 79, pp. 103677, 2022. DOI: [10.1016/j.scs.2022.103677](https://doi.org/10.1016/j.scs.2022.103677).
- [6] M. Hemmat Esfe, "Designing a neural network for predicting the heat transfer and pressure drop characteristics of Ag/water nanofluids in a heat exchanger," *Appl. Therm. Eng.*, vol. 126, pp. 559–565, 2017. DOI: [10.1016/j.applthermaleng.2017.06.046](https://doi.org/10.1016/j.applthermaleng.2017.06.046).
- [7] R. Alizadeh, *et al.*, "A machine learning approach to the prediction of transport and thermodynamic processes in multiphysics systems - heat transfer in a hybrid nanofluid flow in porous media," *J. Taiwan Inst. Chem. Eng.*, vol. 124, pp. 290–306, 2021. DOI: [10.1016/j.jtice.2021.03.043](https://doi.org/10.1016/j.jtice.2021.03.043).
- [8] J. Lu, S. He, J. Ding, J. Yang and J. Liang, "Convective heat transfer of high temperature molten salt in a vertical annular duct with cooled wall," *Appl. Therm. Eng.*, vol. 73, no. 2, pp. 1519–1524, 2014. DOI: [10.1016/j.applthermaleng.2014.05.098](https://doi.org/10.1016/j.applthermaleng.2014.05.098).
- [9] M. M. Alqarni, M. Ibrahim, T. A. Assiri, T. Saeed, A. A. A. Mousa and V. Ali, "Two-phase simulation of a shell and tube heat exchanger filled with hybrid nanofluid," *Eng. Anal. Bound. Elem.*, vol. 146, pp. 80–88, 2023. DOI: [10.1016/j.enganabound.2022.10.001](https://doi.org/10.1016/j.enganabound.2022.10.001).
- [10] Y. Qiu, M. J. Li, W. Q. Wang, B. C. Du and K. Wang, "An experimental study on the heat transfer performance of a prototype molten-salt rod baffle heat exchanger for concentrated solar power," *Energy*, vol. 156, pp. 63–72, 2018. DOI: [10.1016/j.energy.2018.05.040](https://doi.org/10.1016/j.energy.2018.05.040).

- [11] M. W. Ahmad, M. Mourshed and Y. Rezgui, "Trees vs Neurons: comparison between random forest and ANN for high-resolution prediction of building energy consumption," *Energy Build.*, vol. 147, pp. 77–89, 2017. DOI: [10.1016/j.enbuild.2017.04.038](https://doi.org/10.1016/j.enbuild.2017.04.038).
- [12] F. Deng, Y. He, S. Zhou, Y. Yu, H. Cheng and X. Wu, "Compressive strength prediction of recycled concrete based on deep learning," *Constr. Build. Mater.*, vol. 175, pp. 562–569, 2018. DOI: [10.1016/j.conbuildmat.2018.04.169](https://doi.org/10.1016/j.conbuildmat.2018.04.169).
- [13] J. Seo and D. Shin, "Size effect of nanoparticle on specific heat in a ternary nitrate (LiNO₃–NaNO₃–KNO₃) salt eutectic for thermal energy storage," *Appl. Therm. Eng.*, vol. 102, pp. 144–148, 2016. DOI: [10.1016/j.applthermaleng.2016.03.134](https://doi.org/10.1016/j.applthermaleng.2016.03.134).
- [14] H. R. Abbasi, E. Sharifi Sedeh, H. Pourrahmani and M. H. Mohammadi, "Shape optimization of segmental porous baffles for enhanced thermo-hydraulic performance of shell-and-tube heat exchanger," *Appl. Therm. Eng.*, vol. 180, pp. 115835, 2020. DOI: [10.1016/j.applthermaleng.2020.115835](https://doi.org/10.1016/j.applthermaleng.2020.115835).
- [15] A. T. Vu, S. Gulati, P. A. Vogel, T. Grunwald and T. Bergs, "Machine learning-based predictive modeling of contact heat transfer," *Int. J. Heat Mass Transf.*, vol. 174, pp. 121300, 2021. DOI: [10.1016/j.ijheatmasstransfer.2021.121300](https://doi.org/10.1016/j.ijheatmasstransfer.2021.121300).
- [16] M. Jamei, M. Karbasi, I. Adewale Olumegbon, M. Mosharaf-Dehkordi, I. Ahmadianfar and A. Asadi, "Specific heat capacity of molten salt-based nanofluids in solar thermal applications: a paradigm of two modern ensemble machine learning methods," *J. Mol. Liq.*, vol. 335, pp. 116434, 2021. DOI: [10.1016/j.molliq.2021.116434](https://doi.org/10.1016/j.molliq.2021.116434).
- [17] J. Fan, *et al.*, "Comparison of support vector machine and extreme gradient boosting for predicting daily global solar radiation using temperature and precipitation in humid subtropical climates: a case study in China," *Energy Convers. Manag.*, vol. 164, pp. 102–111, 2018. DOI: [10.1016/j.enconman.2018.02.087](https://doi.org/10.1016/j.enconman.2018.02.087).
- [18] A. Karimipour, S. A. Bagherzadeh, A. Taghipour, A. Abdollahi and M. R. Safaei, "A novel nonlinear regression model of SVR as a substitute for ANN to predict conductivity of MWCNT-CuO/water hybrid nanofluid based on empirical data," *Phys. A Stat. Mech. Appl.*, vol. 521, pp. 89–97, 2019. DOI: [10.1016/j.physa.2019.01.055](https://doi.org/10.1016/j.physa.2019.01.055).
- [19] H. T. Bang, S. Yoon and H. Jeon, "Application of machine learning methods to predict a thermal conductivity model for compacted bentonite," *Ann. Nucl. Energy*, vol. 142, pp. 107395, 2020. DOI: [10.1016/j.anucene.2020.107395](https://doi.org/10.1016/j.anucene.2020.107395).
- [20] A. Marani and M. L. Nehdi, "Machine learning prediction of compressive strength for phase change materials integrated cementitious composites," *Constr. Build. Mater.*, vol. 265, pp. 120286, 2020. DOI: [10.1016/j.conbuildmat.2020.120286](https://doi.org/10.1016/j.conbuildmat.2020.120286).
- [21] L. Zhou, D. Garg, Y. Qiu, S. M. Kim, I. Mudawar and C. R. Kharangate, "Machine learning algorithms to predict flow condensation heat transfer coefficient in mini/micro-channel utilizing universal data," *Int. J. Heat Mass Transf.*, vol. 162, pp. 120351, 2020. DOI: [10.1016/j.ijheatmasstransfer.2020.120351](https://doi.org/10.1016/j.ijheatmasstransfer.2020.120351).
- [22] O. Acikgoz, A. B. Çolak, M. Camci, Y. Karakoyun and A. S. Dalkilic, "Machine learning approach to predict the heat transfer coefficients pertaining to a radiant cooling system coupled with mixed and forced convection," *Int. J. Therm. Sci.*, vol. 178, pp. 107624, 2022. DOI: [10.1016/j.ijthermalsci.2022.107624](https://doi.org/10.1016/j.ijthermalsci.2022.107624).
- [23] B. Kwon, F. Ejaz and L. K. Hwang, "Machine learning for heat transfer correlations," *Int. Commun. Heat Mass Transf.*, vol. 116, pp. 104694, 2020. DOI: [10.1016/j.icheatmasstransfer.2020.104694](https://doi.org/10.1016/j.icheatmasstransfer.2020.104694).
- [24] A. Shahsavari, A. Goodarzi, I. Baniasad Askari, M. Jamei, M. Karbasi and M. Afrand, "The entropy generation analysis of the influence of using fins with tip clearance on the thermal management of the batteries with phase change material: application of a new gradient-based ensemble machine learning approach," *Eng. Anal. Bound. Elem.*, vol. 140, pp. 432–446, 2022. DOI: [10.1016/j.enganabound.2022.04.024](https://doi.org/10.1016/j.enganabound.2022.04.024).
- [25] R. Alizadeh, J. Mohebbi Najm Abad, A. Fattahi, E. Alhajri and N. Karimi, "Application of machine learning to investigation of heat and mass transfer over a cylinder surrounded by porous media—The radial basic function network," *J. Energy Resour. Technol. Trans. ASME*, vol. 142, no. 11, pp. 1–12, 2020. DOI: [10.1115/1.4047402](https://doi.org/10.1115/1.4047402).
- [26] S. Lu, Q. Li, L. Bai and R. Wang, "Performance predictions of ground source heat pump system based on random forest and back propagation neural network models," *Energy Convers. Manag.*, vol. 197, pp. 111864, 2019. DOI: [10.1016/j.enconman.2019.111864](https://doi.org/10.1016/j.enconman.2019.111864).
- [27] Y. Li, *et al.*, "Random forest regression for online capacity estimation of lithium-ion batteries," *Appl. Energy*, vol. 232, pp. 197–210, 2018. DOI: [10.1016/j.apenergy.2018.09.182](https://doi.org/10.1016/j.apenergy.2018.09.182).
- [28] M. W. Ahmad, M. Mourshed and Y. Rezgui, "Tree-based ensemble methods for predicting PV power generation and their comparison with support vector regression," *Energy*, vol. 164, pp. 465–474, 2018. DOI: [10.1016/j.energy.2018.08.207](https://doi.org/10.1016/j.energy.2018.08.207).
- [29] S. H. Godasiaei and A. J. Chamkha, "Numerical heat transfer, Part A : applications advancing heat transfer modeling through machine learning: a focus on forced convection with nanoparticles," *Numer. Heat Transf. Part A Appl.*, pp. 1–23, 2024. DOI: [10.1080/10407782.2023.2299734](https://doi.org/10.1080/10407782.2023.2299734).

- [30] A. Torres-Barrán, Á. Alonso and J. R. Dorronsoro, "Regression tree ensembles for wind energy and solar radiation prediction," *Neurocomputing*, vol. 326–327, pp. 151–160, 2019. DOI: [10.1016/j.neucom.2017.05.104](https://doi.org/10.1016/j.neucom.2017.05.104).
- [31] W. Li, Y. Yin, X. Quan and H. Zhang, "Gene expression value prediction based on XGBoost algorithm," *Front Genet*, vol. 10, pp. 1077, 2019. DOI: [10.3389/fgene.2019.01077](https://doi.org/10.3389/fgene.2019.01077).
- [32] Z. Said, P. Sharma, B. J. Bora and A. K. Pandey, "Sonication impact on thermal conductivity of f-MWCNT nanofluids using XGBoost and Gaussian process regression," *J. Taiwan Inst. Chem. Eng.*, vol. 145, pp. 104818, 2023. DOI: [10.1016/j.jtice.2023.104818](https://doi.org/10.1016/j.jtice.2023.104818).
- [33] P. Sharma, *et al.*, "Recent Advances in Machine Learning Research for Nanofluid-Based Heat Transfer in Renewable Energy System," *Energy Fuel.*, vol. 36, no. 13, pp. 6626–6658, 2022. DOI: [10.1021/acs.energyfuels.2c01006](https://doi.org/10.1021/acs.energyfuels.2c01006).
- [34] J. Tang, S. Yu, C. Meng, H. Liu and Z. Mo, "Prediction of heat transfer of bubble condensation in sub-cooled liquid using machine learning methods," *Chem. Eng. Sci.*, vol. 271, pp. 118578, 2023. DOI: [10.1016/j.ces.2023.118578](https://doi.org/10.1016/j.ces.2023.118578).
- [35] K. N. Çerçi and M. Daş, "Modeling of heat transfer coefficient in solar greenhouse type drying systems," *Sustain*, vol. 11, no. 18, pp. 5127, 2019. DOI: [10.3390/su11185127](https://doi.org/10.3390/su11185127).
- [36] P. Sharma, K. Ramesh, R. Parameshwaran and S. S. Deshmukh, "Thermal conductivity prediction of titania-water nanofluid: a case study using different machine learning algorithms," *Case Stud. Therm. Eng.* vol. 30, pp. 101658, 2022. DOI: [10.1016/j.csite.2021.101658](https://doi.org/10.1016/j.csite.2021.101658).
- [37] A. Subasi, E. Alickovic and J. Kevric, "Diagnosis of Chronic Kidney Disease by Using Random Forest", *Cmbebih* 2017, vol. 62, 2017. DOI: [10.1007/978-981-10-4166-2](https://doi.org/10.1007/978-981-10-4166-2).
- [38] S. M. Ekranı, S. Ganjehzadeh and J. A. Esfahani, "Multi-objective optimization of a tubular heat exchanger enhanced with delta winglet vortex generator and nanofluid using a hybrid CFD-SVR method," *Int. J. Therm. Sci.*, vol. 186, pp. 108141, 2023. DOI: [10.1016/j.ijthermalsci.2023.108141](https://doi.org/10.1016/j.ijthermalsci.2023.108141).
- [39] B. C. Du, Y. L. He, K. Wang and H. H. Zhu, "Convective heat transfer of molten salt in the shell-and-tube heat exchanger with segmental baffles," *Int. J. Heat Mass Transf.*, vol. 113, pp. 456–465, 2017. DOI: [10.1016/j.ijheatmasstransfer.2017.05.075](https://doi.org/10.1016/j.ijheatmasstransfer.2017.05.075).
- [40] Y. L. He, Z. J. Zheng, B. C. Du, K. Wang and Y. Qiu, "Experimental investigation on turbulent heat transfer characteristics of molten salt in a shell-and-tube heat exchanger," *Appl. Therm. Eng.*, vol. 108, pp. 1206–1213, 2016. DOI: [10.1016/j.applthermaleng.2016.08.023](https://doi.org/10.1016/j.applthermaleng.2016.08.023).
- [41] B. C. Du, Y. L. He, Y. Qiu, Q. Liang and Y. P. Zhou, "Investigation on heat transfer characteristics of molten salt in a shell-and-tube heat exchanger," *Int. Commun. Heat Mass Transf.*, vol. 96, pp. 61–68, 2018. DOI: [10.1016/j.icheatmasstransfer.2018.05.020](https://doi.org/10.1016/j.icheatmasstransfer.2018.05.020).
- [42] S. He, J. Lu, J. Ding, T. Yu and Y. Yuan, "Convective heat transfer of molten salt outside the tube bundle of heat exchanger," *Exp. Therm. Fluid Sci.*, vol. 59, pp. 9–14, 2014. DOI: [10.1016/j.expthermflusci.2014.07.008](https://doi.org/10.1016/j.expthermflusci.2014.07.008).
- [43] C. A. Ramezan, T. A. Warner and A. E. Maxwell, "Evaluation of sampling and cross-validation tuning strategies for regional-scale machine learning classification," *Remote Sens.*, vol. 11, no. 2, pp. 185, 2019. DOI: [10.3390/rs11020185](https://doi.org/10.3390/rs11020185).
- [44] C. Bergmeir and J. M. Benítez, "On the use of cross-validation for time series predictor evaluation," *Inf. Sci. (Ny.)*, vol. 191, pp. 192–213, 2012. DOI: [10.1016/j.ins.2011.12.028](https://doi.org/10.1016/j.ins.2011.12.028).
- [45] R. D. King, O. I. Orhobor and C. C. Taylor, "Cross-validation is safe to use," *Nat Mach Intell*, vol. 3, no. 4, pp. 276–276, 2021. DOI: [10.1038/s42256-021-00332-z](https://doi.org/10.1038/s42256-021-00332-z).
- [46] A. Ashrafian, F. Shokri, M. J. Taheri Amiri, Z. M. Yaseen and M. Rezaie-Balf, "Compressive strength of foamed cellular lightweight concrete simulation: new development of hybrid artificial intelligence model," *Constr. Build. Mater.*, vol. 230, pp. 117048, 2020. DOI: [10.1016/j.conbuildmat.2019.117048](https://doi.org/10.1016/j.conbuildmat.2019.117048).
- [47] Z. M. Yaseen, *et al.*, "Predicting compressive strength of lightweight foamed concrete using extreme learning machine model," *Adv. Eng. Softw.*, vol. 115, pp. 112–125, 2018. DOI: [10.1016/j.advengsoft.2017.09.004](https://doi.org/10.1016/j.advengsoft.2017.09.004).
- [48] B. A. Young, A. Hall, L. Pilon, P. Gupta and G. Sant, "Can the compressive strength of concrete be estimated from knowledge of the mixture proportions?: New insights from statistical analysis and machine learning methods," *Cem. Concr. Res.*, vol. 115, pp. 379–388, 2019. DOI: [10.1016/j.cemconres.2018.09.006](https://doi.org/10.1016/j.cemconres.2018.09.006).
- [49] Z. M. Yaseen, B. Keshtegar, H. J. Hwang and M. L. Nehdi, "Predicting reinforcing bar development length using polynomial chaos expansions," *Eng. Struct.*, vol. 195, pp. 524–535, 2019. DOI: [10.1016/j.engstruct.2019.06.012](https://doi.org/10.1016/j.engstruct.2019.06.012).